Remote Sensing of Environment 121 (2012) 51–60

Contents lists available at SciVerse ScienceDirect

Remote Sensing of Environment

journal homepage: www.elsevier.com/locate/rse

Retrieving sand dune movements using sub-pixel correlation of multi-temporal optical remote sensing imagery, northwest Sinai Peninsula, Egypt

ElSayed Hermas [a,*], Sebastien Leprince [b], Islam Abou El-Magd [c]

[a] Geography Department, Umm Al-Qura University, Makkah, Saudi Arabia
[b] California Institute of Technology, California, USA
[c] The National Authority of Remote Sensing and Space Sciences, Cairo, Egypt

ARTICLE INFO

Article history:
Received 24 August 2011
Received in revised form 17 December 2011
Accepted 7 January 2012
Available online 17 February 2012

Keywords:
Sand dune movement
Sinai Peninsula
Optical remote sensing
COSI-Corr

ABSTRACT

Sand dune movements pose potential hazards against various land use activities in Egypt. To avoid or to minimize the hazards associated with sand dunes, it is critical to determine their rates and patterns of migration at high accuracy and over wide spatial coverage. This is, however, a real challenge using field work and traditional remote sensing approaches. The co-registration of optically sensed images and correlation (COSI-Corr) complements traditional approaches to provide accurate measurements at wide spatial coverage. Applying the COSI-Corr technique to two SPOT 4 panchromatic images acquired above North Sinai, we measured lateral migration of 6.0 to 19.4 m/yr with an average of 7.7 m/yr, and 9.3 to 15.0 m/yr with an average of 11.9 m/yr for the whole barchans dune areas and a selected sample of barchan dunes, respectively. We also detected that the lateral movements along the crest lines of linear dunes ranged from 4.0 to 20.1 m/yr with an average of 6.8 m/yr for the whole area occupied by linear dunes. For a selected linear dune within the study area, the lateral migration of peaks and saddles along the crest lines ranged from 5.5 to 16.7 m/yr with an average of 12.4 m/yr. The lateral migration of both barchans dunes and linear dunes showed high spatial variability. Validation of these results against the previously measured migration rates indicated high degree of accuracy of the technique. In addition, the displacement field produced from the correlation indicated that the direction of sand dune movements occurred towards the east and southeast, which is well aligned with the previously determined sand dune drifting potentials.

1. Introduction

The dynamic of landscapes is controlled by various Earth surface processes and human activities. One of the dynamic Earth surface processes in north Sinai is the aeolian process, which produces vast areas of sand dunes. Under arid conditions where the evaporation rates exceed the precipitation rates and the vegetation cover is scarce, sand dunes move at various rates and directions. Determination of sand dune migration rates and their spatial variability became a necessity for the conservation of both natural resources and man-made projects. Until now, there has been no mature methodology to detect and measure the movement of sand dunes at fine spatial and temporal resolutions, and over wide spatial coverage (Liu et al., 1997).

Previous researches on the detection and measurement of sand dune migration in north Sinai have followed two techniques: the ground-based techniques and the remote sensing-based techniques. The ground based techniques include linen tape (Misak & ElShazly, 1982), and steel, iron, plastic rods, and total station along with GPS (Aql, 2002; Asal, 1999; ElBanna, 2004; ElDessouki, 2000; ElKayali, 1984; Khidr, 2006; Mounir, 1983; Tsoar, 1978). Although these techniques show high level of accuracy, they provided measurements on localized sand dunes at monthly or seasonal intervals. Since they rely on targeted field measurements, these methods inherently lack the capability to monitor dune migration at wide spatial coverage. In addition, they are expensive and time consuming. The classical remote sensing techniques for monitoring sand dune migration are typically carried out by comparing multi-temporal aerial photographs or satellite images (Aql, 2002; ElBanna, 2004; Tsoar, 1978; Tsoar et al., 2004). Unlike field measurements, remotely sensed data show regular and wide coverage for analysis and measurement. Aerial photographs are, however, expensive, and analyzing them manually is time consuming. Furthermore, although satellite imagery provides multi-temporal coverage of large areas at lower cost, the classical definition of sand dune boundaries is highly affected by satellite geometry, sensor parameters, and illumination conditions in addition to personal bias through the process of visually tracing dune boundaries. These challenges make the determination of sand dune movements from satellite images difficult (Liu et al., 1997). Developing a new technique that fills in the gaps of the previously mentioned techniques is required.

* Corresponding author at: Geography Department, Faculty of Social Sciences, Umm Al-Qura University, Makkah, Saudi Arabia. Tel.: +966 252 70 000, +966 546 033 870 (mobile).
E-mail address: eaibrahim@uqu.edu.sa (E. Hermas).

0034-4257/$ – see front matter © 2012 Elsevier Inc. All rights reserved.
doi:10.1016/j.rse.2012.01.002

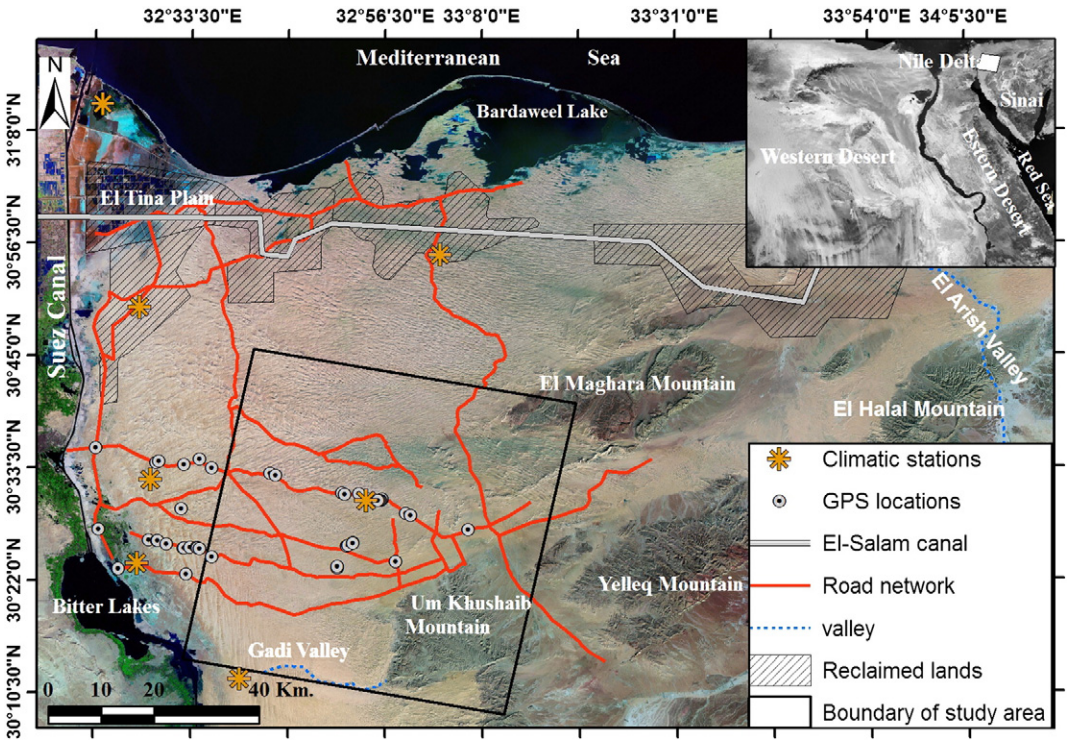

Fig. 1. Location map of the study area.

The Co-registration of Optically Satellite Imagery and Correlation (COSI-Corr) (Leprince et al., 2007) could be a potential alternative technique for the detection and the measurement of sand dune migration. The technique has essentially been developed to detect and measure the subtle crustal deformation in tectonically active areas with high level of accuracy (Avouac et al., 2006; Ayoub et al., 2009; Leprince et al., 2007; Liu et al., 2006; Schiek, 2004; Schiek & Hurtado, 2006; Van Puymbroeck et al., 2000). Few studies had been conducted on the dynamics of Earth surface processes using this technique such as glacier processes (Scherler et al., 2008) and dune movements (Necsoiu et al., 2009; Vermeesch & Drake, 2008). The main goal of this paper is to apply the COSI-Corr technique using two SPOT 4 panchromatic images to detect dune displacement at subpixel accuracy, over wide spatial coverage of the northwest Sinai Peninsula, and validate the results against previous measurements of both magnitude and direction of dune movements.

2. Study area

The study area is located in the northwestern corner of the Sinai Peninsula (Fig. 1). It is bounded from the North by El-Tina Plain and Lake Bardweel; to the south by the trunk valley of Wadi Gadi and Um Khushaib Mountain; to the east by El-Maghara, and Yelleq mountains; and to the west by Suez Canal and Bitter Lake (Fig. 1). The climate of the study area is typically arid (ElBanna, 2004) where the rates of evaporation exceed the rates of precipitation, which does not exceed 28.0 mm yr^{-1} (Aql, 2002). The annual minimum average temperature is ~14.0 °C whereas the annual maximum average temperature is ~40.0 °C. The high temperatures and low rainfalls through most of the year minimize the opportunity for plant cover to grow over sand dunes in North Sinai, and provide the conditions for the formation and movements of sand dunes (Aql, 2002; ElBanna, 2004; ElDessouki, 2000).

North Sinai is considered one of the main target areas for lateral expansion of various development projects. Indeed, 1680 Km^2 were allocated for various agricultural projects. Various infrastructures were developed such as paved roads and railways networks along with many artificial irrigation channels. The threat of sand dune encroachment against the already established man-made activities had been documented and reported (Aql, 2002; ElBanna, 2004; ElDessouki, 2000; Khidr, 2006) (Fig. 2). Although north Sinai represents a vast field of sand dunes, limited studies have been conducted on the migration of these dunes, in particular linear dunes that represent the main aeolian form in north Sinai. It is therefore necessary to

Fig. 2. Encroachment of sand dunes against roads in the study area.

Table 1
The specifications of the panchromatic level 1A SPOT 4 images used in the study.

SPOT 4	Date	Spatial resolution	Viewing angle	Sun elevation	Cloud cover
Master image	May 25, 2007	10.0	8.6	71.4°	0.0
Slave image	Jan. 14, 2008	10.0	8.6	34.1°	0.0

develop a methodology to map sand dune dynamics in north Sinai at high level of accuracy and over wide spatial coverage to define the safe corridors and patches that sustain these projects and their infrastructures.

3. Methodology

The COSI-Corr (Coregistration of Optically Sensed Images and Correlation, Leprince et al., 2007) technique was used in this research to detect and measure sand dune movement. Two SPOT 4 L1A Panchromatic images at 10 m ground resolution were acquired to conduct the COSI-Corr technique: the master image was acquired in May 2007, and the slave image in January 2008. These two images have low and similar incidence angles to minimize stereoscopic effects (Michel and Avouac, 2002; Schiek, 2004; Van Puymbroeck et al., 2000). The technical specifications of these images are provided in Table 1. The pre-processing step involved ortho-rectification and co-registration processes of the May 2007 and January 2008 images. The ortho-rectification started by careful selection of the tie points between a previously ortho-rectified image and a slave image (the raw image). The tie points were selected at the intersection between road and stream networks available in the study. These tie points were then converted into GCP's, and eventually optimized using the reference image, a free sinks SRTM DEM (90 m spatial resolution). The COSI-Corr Fourier correlation engine was used to correlate the first ortho-rectified image (May 2007) with the second ortho-rectified image (January 2008). Various frequency correlator engine parameters were tested. The best result in our case was obtained using the frequency correlation with window sizes 32-to-16 pixels and a shifting step with size of 2 pixels. The correlation process produced a horizontal displacement image composed of three components: east–west, north–south, and signal-to-noise ratio (SNR) (Fig. 3). Various decorrelation measurements are represented in the produced correlation image, and represented either by low, null, or extreme ± unphysical measurements in the correlation images. The decorrelation measurements represented 0.14% of the entire image. These values are associated with various noise sources such as alluvions and/or the topographic shadowing differences, eroded hills, and alluvial deposits along with the mountainous areas. The outliers outside the range of ±20 m were discarded and remaining values were denoised using the Non-Local Means filter (Buades et al., 2008; User's Guide to COSI-Corr, 2009). The statistics of the filtered correlation image indicated a Gaussian distribution (Fig. 3), and the mean values of pixel displacement in both the east–west and the north–south images are 5.6 cm and 32.1 cm respectively with a common average of 18.8 cm. This average indicated that a registration better than 1/50 of the nominal spatial resolution of the used images was performed. Both the east–west and north–south displacement components were used following the approach presented by Necsoiu et al. (2009) to calculate the

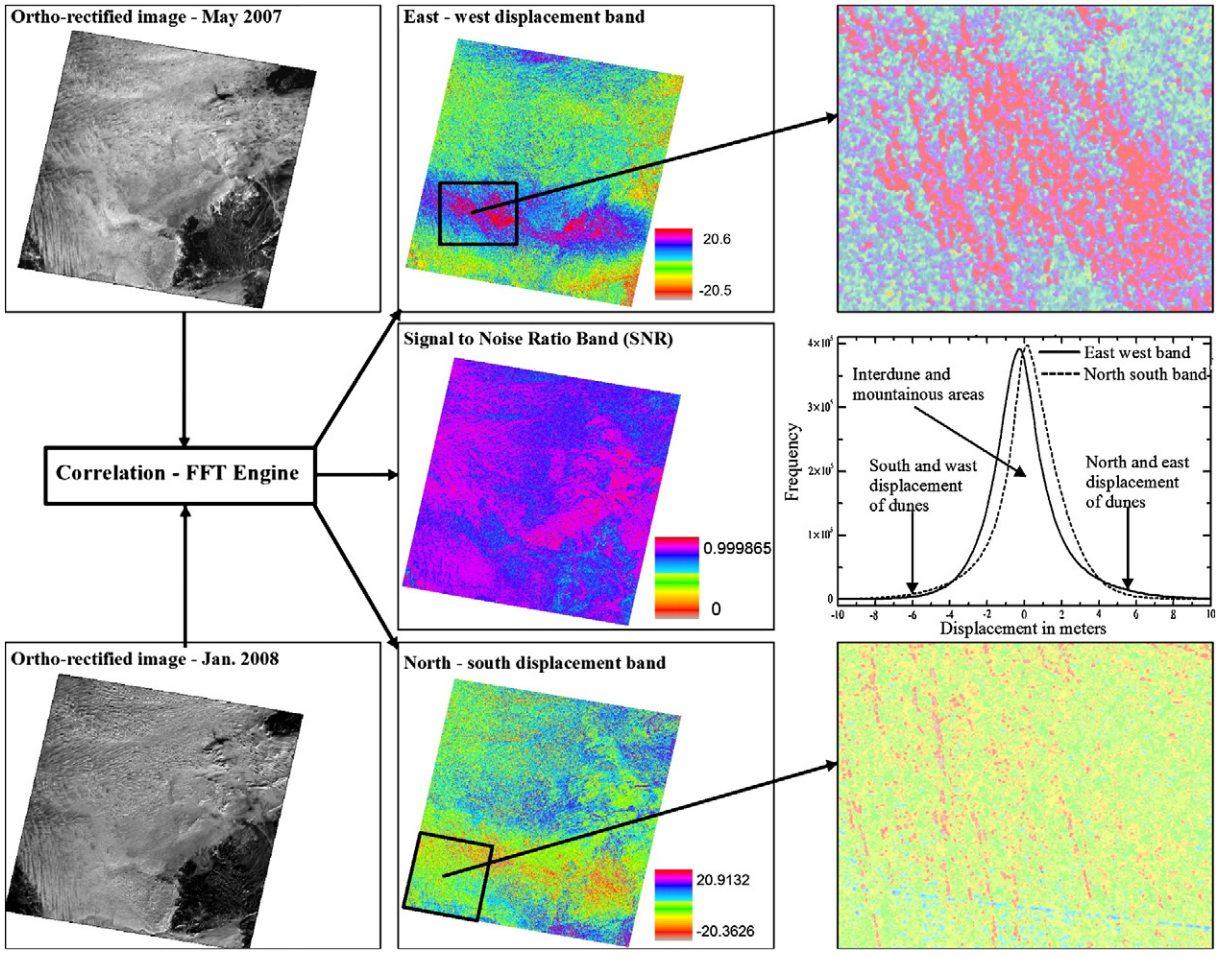

Fig. 3. The main steps of producing the displacement images.

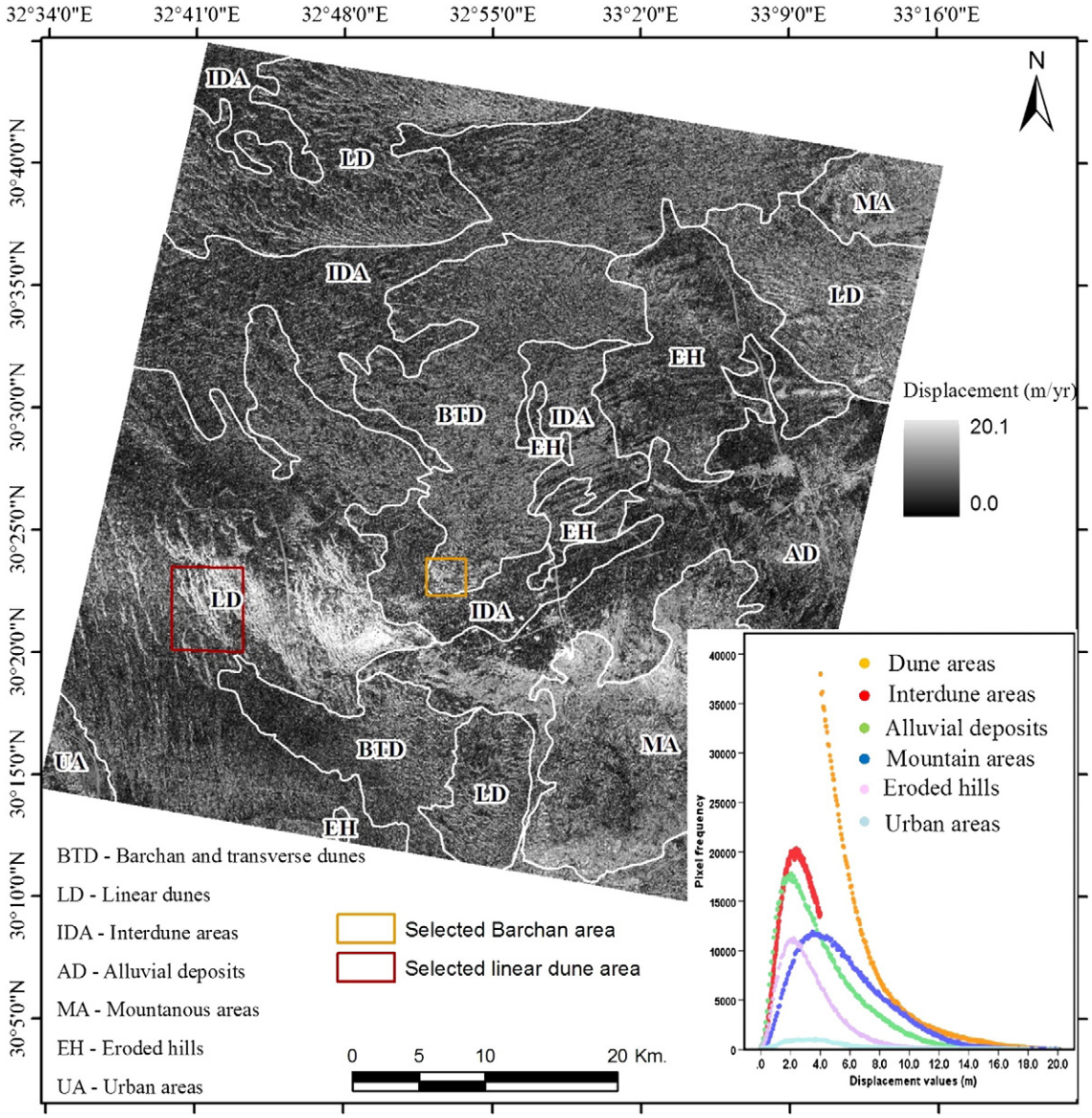

Fig. 4. The various morphologic units overlain on the calculated net annual displacement image along with a graph showing the frequency of pixel displacement of each unit. Boxes represent the studied dune fields in Figs. 6, 7, and 10.

net pixel displacement in the study area through the 229 days. These values were scaled to 365 days to derive the annual net pixel displacements. In addition, both the east–west and the north–south components of the displacement were used to produce 2-D vector displacement field. In addition, a two-day field work was carried out to support the results of the technique.

4. Results and discussion

4.1. Spatial distribution against pixel displacement

Aeolian landforms are major morphologic components in north Sinai, and comprise a variety of sand dunes including barchans, transverse, and

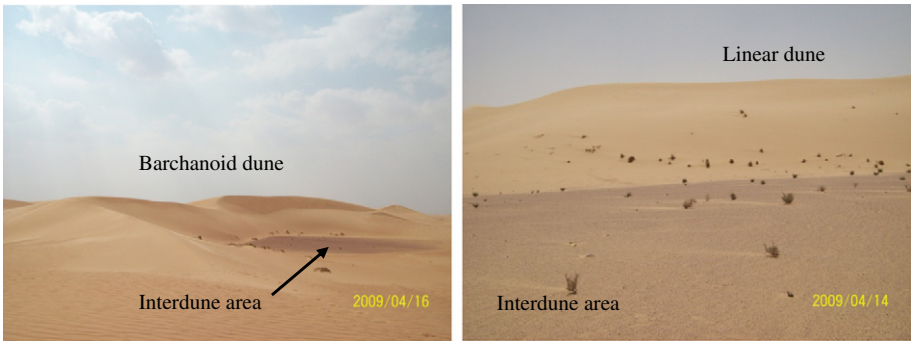

Fig. 5. Barchanoid and linear dunes against interdune area.

linear dunes. As an arid region, the linear dunes dominate (Tsoar, 1978) which represent the majority of the aeolian landforms in the study area (Fig. 4). To the east, and next to the mountainous regions where one directional wind prevail, the barchans and transverse dunes dominate (Fig. 4). Barchan dunes occur either as scattered dunes or coalesced together forming the barchanoid dunes as a transitional step to be linear dunes (Aql, 2002; Bagnlod, 1941; ElBanna, 2004; ElDessouki, 2000; Khidr, 2006; Tsoar, 1984, 1989) (Fig. 5). Most of these dunes, in particular the linear dunes, occur as longitudinal belts overlying the older sand sheets that occupy the interdune areas (Fig. 5). The interdune areas are undulating low topographic surfaces that are represented by streaked and deflated sand sheets (Khalaf et al., 1998), and trend, in most of the cases, in the NW–SE direction. The spatial distribution and pattern of both the dune and the interdune areas are characterized by the spatial variability of the magnitude of the calculated net annual pixel displacements (Fig. 4). The interdune areas are generally considered stable lands that do not show tangible movements whereas the various forms of sand dunes move at variable rates and in various directions. This is demonstrated by the relative spatial variability of the pixel displacement values of both sand dune and interdune areas (Fig. 4). The pixel displacement of the entire areas occupied by sand dunes range from 4.0 to 20.0 m with an average of 6.6 m whereas the pixel displacements of the interdune areas are in the order of 0.0 to 4.0 with a net average of 2.4 m. Along with the dune and interdune areas, other morphologic units are represented in the study area which are the eroded hills, mountainous areas, and alluvial deposits in the east of the study area. In the southwest, some urban areas are represented as well. The pixel displacements of the eroded hills range from 0.0 to 19.4 m with a net average of 3.3 m (Fig. 4). The pixel displacement values of the alluvial deposits ranged from 0.0 to 20.1 m with a net average 4.0 m. In the mountainous areas, the pixel displacements ranged from 0.0 to 20.1 m with an average of 5.5 m. Finally, the values of the pixel displacements of the urban areas located in the southwest range from 0.0 to 20.0 m with an average of 4.1 m. Studying the distribution of pixel displacements for the various morphologic (Fig. 4) indicated that the mean of all the morphologic units is highly affected by the high noise values at the right end of the graph. These values may be inherited from the different sources noise from the images. However, the pixel displacement values of the calculated net annual image provided a reasonable estimation of the magnitude and direction of dune displacements in the study area as it is shown in the next sections.

4.2. Magnitude of sand dunes' movements

The migration rates of different dune forms at different locations in north Sinai were measured using various techniques (Tables 2 and 3). Some of these measurements were carried out on dunes inside the study area; however, the majority is located outside the study area especially in the southern reaches of the coastal area of north Sinai (ElKayali, 1984; Misak & ElShazly, 1982; Mounir, 1983; Tsoar, 1974). As a result of their small sizes and their high rates of migration (Khidr, 2006), the majority of the measurements were conducted on barchan dunes using field techniques. Very limited studies were carried out using remote sensing.

Table 2
The average migration rates of barchan dunes as recorded in the previous works.

Authors	Dune type	Technique	LMBD (m/yr)
Tsoar (1974)	Barchan	Field techniques	8.6
Misak and ElShazly (1982)	Barchan	Linen tape	13.3
Mounir (1983)	Barchan	Wood and steel posts	13.8
ElKayali (1984)	Barchan	Steel and wood rods	17.3
Asal (1999)	Barchan	Steel posts	4.0
ElBanna (1999)	Barchan	Field techniques	13.5
Hereher (2000)	Barchan	Wilson model 1972	8.8
Aql (2002)	Barchan	Steel posts	13.4
ElBanna (2004)	Barchan	Total station	3.5
	Barchans	Remote sensing	3.6

LMBD, Lateral migration of barchan dunes.

Table 3
The average migration rates of linear dunes as recorded from the previous studies.

Authors	Technique	LMLD (m/yr)	EMLD (m/yr)	LOLD (m/yr)
Tsoar (1978)	Field technique	6.0	14.5	8.4
	Remote sensing	–	–	7.5
Tsoar, 1983	Field technique	–	14.7	8.2
Asal (1999)	Field technique	6.0	13.0	–
	Field technique	4.5	8.5	–
ElDessouki (2000)	Field technique	–	10.0	–
ElBanna (2004)	Field technique	0.7 and 2.0	2.3 and 13.0	–
	Remote sensing	–	–	10.9
Tsoar et al. (2004)	Remote sensing	3.8–5.8	–	–
	Field technique	6.1–7.5	–	–
Khidr (2006)		10.6	27.0	–

LMLD, Lateral movements of linear dunes; EMLD, Elongation movements of linear dunes;
LOLD, Longitudinal movements of linear dunes.

Tsoar (1974) used field techniques to measure the migration rates of three crescentic dunes of different heights at El-Arish region along the Mediterranean coast. The migration rates of these barchans dunes vary from 6.16, 6.42, to 13.08 m/yr with an average of 8.6 m/yr. Misak and ElShazly (1982) used the linen tape at El-Arish area and estimated a migration rate of a barchans dune over nine months to be 13.3 m/yr. Mounir (1983) studied fourteen barchan dunes south the Mediterranean coast (north Sinai) through a three months time period (January–March 1983) and estimated migration rates in the order of 0.9 to 6.0 m with an average of 13.8 m/yr. ElKayali (1984) measured the migration rates at Bir Al Musama (north Sinai) over nine months time period for a two sets of barchans dunes: a set of small sizes and another set of relatively large sizes. The small set of the barchans dunes migrates at a rate of 16.0 m/yr whereas the migration rate of the large barchans dunes was 10.0 m/yr with an average of 17.3 m/yr. Asal (1999) studied two barchan dunes at El Sadat area (north Sinai) using field technique, and estimated a migration rate ranging from 6.0 to7.0 m/yr for the small one and 1.5 m/yr for the larger one with an average of 4.0 m/yr. Aql (2002) established wood posts on a barchans dune west of the study area and measured the movement of dune each three months through the time period June 2001 to June 2002. The rate of the recorded movements was 13.4 m/yr. ElBanna (2004) used the total station and steel posts to measure the migration rate of a barchans dune just beside the study area. The measurements were carried out monthly and estimated a migration rate of 3.5 m/yr. In addition to the various types of field techniques, Hereher (2000) used the Wilson Model (1972) to measure the advance rate of seven barchans dunes: some inside the study area and other outside the study area. The estimated rates of movements ranged from 5.6 to 13.3 m/yr with an average of 8.8 m/yr. ElBanna (2004) compared an aerial photograph acquired in 1958 with a LandSat TM image acquired in 1998 to measure the displacement of a number of barchan dunes located northwest of the study area. He estimated migration rates of barchans dunes in the order of 1.1 m/yr to 6.8 m/yr. Table (2) demonstrated a wide range of migration rates which vary from 3.5 to 17.3 m/yr with a net average of ~10.0 m/yr. The wide range of the previously measured migration rates may be attributed to the different locations of the targeted dunes, size of the dunes, the spatial variability of wind magnitudes, the length of measurement period, and time interval of measurement (monthly or seasonally), along with the conduction of different techniques. In the study area, barchan dunes are located west of the mountain regime (Fig. 4).

Pixel displacements of the whole area occupied by dunes are on the order of 6.0 to 19.4 m/yr with a net average of 7.7 m/yr. Fig. (6I) represents a selected field of barchans dunes which differentiates

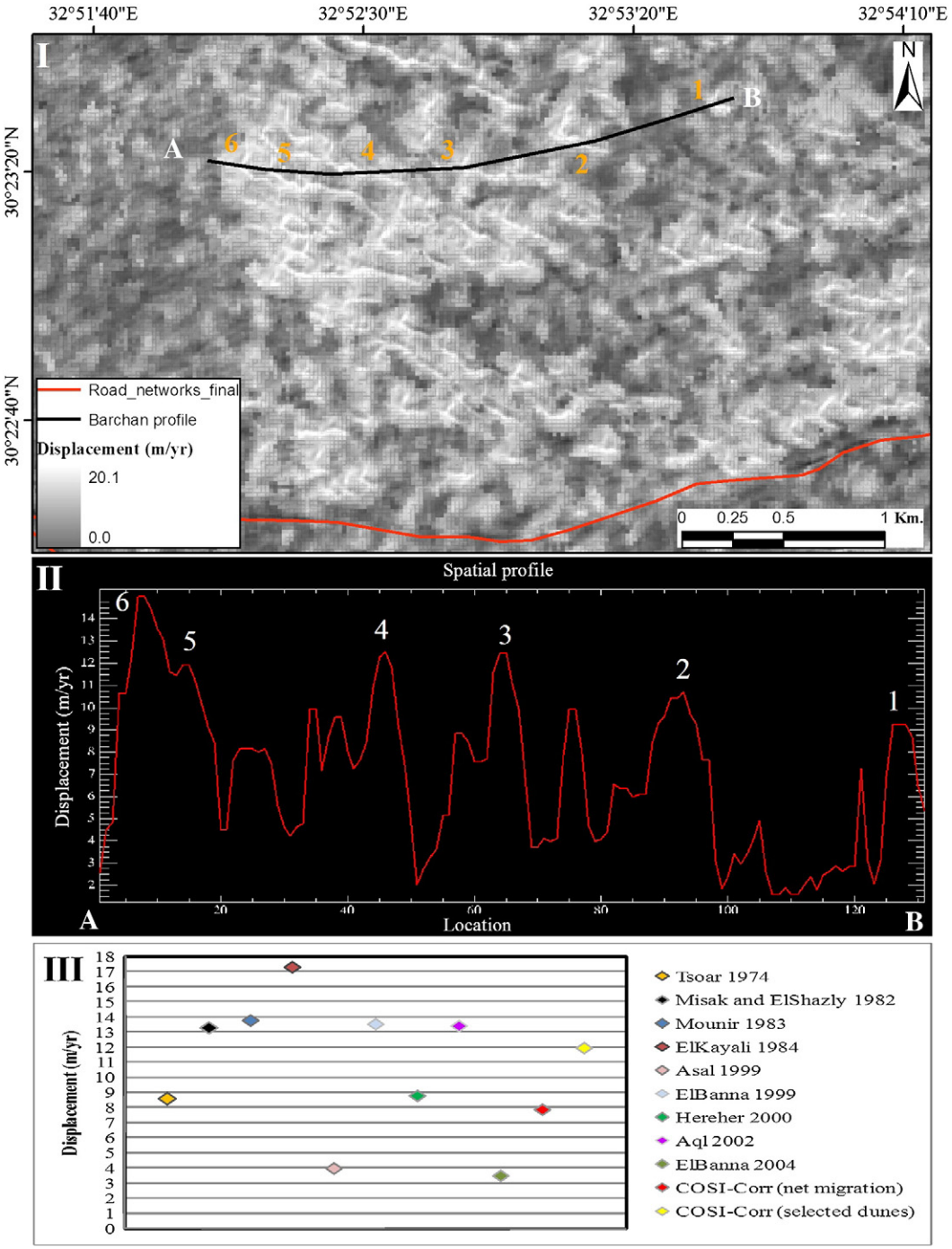

Fig. 6. The net lateral pixel displacement of a selected barchans dune field (I), lateral A–B profile along a selected barchans dunes, and validation against the previous measurements.

clearly the barchan dunes from the interdune areas where the high values of pixel displacement are associated with dunes areas whereas the low displacements values are associated with the interdune areas. The spatial variability of the migration rates among barchan dunes and their characterization from the interdune areas are shown over a 2.6 km long transect (Fig. 6II); a result that is supported by the recorded high spatial variability of the migration rates from the previous studies on the barchans dunes in north Sinai (Table 2). From the selected sample in Fig. (6II), the lateral migration of the dune crest varies from 9.3 to 15.0 m/yr with an average of 11.9 m/yr. Both the net pixel displacement of the entire areas occupied by barchan dunes and the pixel displacement of the selected field of barchan dunes were plotted against the previously measured migration rates in north Sinai (Fig. 6III). This figure indicates that the migration rates calculated by the current technique are located within the range of the previously measured migration rates of barchan dunes. However, the current technique allows to measure, on a pixel-wise scale, the migration rates over wider spatial coverage. In addition to the migration characteristics of the barchans dunes, particular emphasis had been paid to the movements of the linear dunes.

Linear dunes are formed in response to a bi-directional wind regime (Tsoar, 1978; Tsoar, 1983; Tsoar et al., 2004). Both wind regime encounter the linear seif dune at an acute angle, and results in erosion on the windward side. On the leeward side, winds are deflected to form eddies, and allow not only deposition on this side but also erosion as a result of moving sand grains parallel to the crest lines

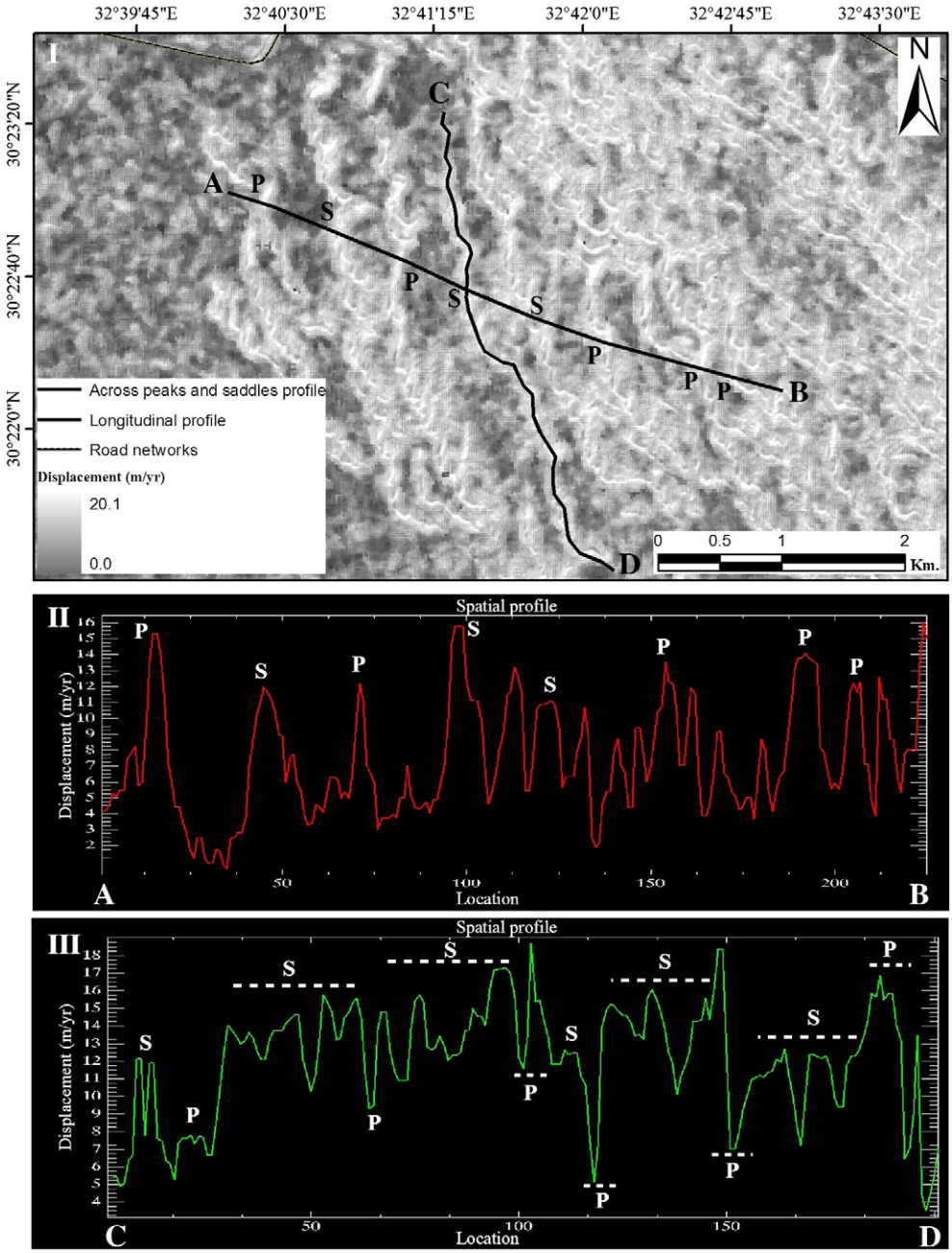

Fig. 7. The net lateral pixel displacement of a selected linear dune field (I), lateral A–B profile along different linear dunes, and longitudinal profile of a selected linear dune.

(Madigan, 1946; Tsoar, 1978, 1983; Tsoar et al., 2004). This process minimizes or prevents the lateral movements of the whole linear dunes. Because the two winds are not uniform in their incidence angles and magnitudes, peaks and saddles are formed along the crest line of the linear dunes (Tsoar, 1978, 1983; Tsoar et al., 2004). Under the influence of this process, the peaks and saddles are displaced along the alignment of the linear dune. At the end of the linear dune, a slip-face is formed that allows the deposition process to dominate, and eventually elongation of the linear dune takes place (Tsoar, 1978). Accordingly, the linear dunes are characterized by a complicated set of movements which are the extension of the dune (elongation), longitudinal displacement of the summits (peak and saddles), and transverse shift in response to the transverse component of the crosswinds (Bagnlod, 1941). In a desert environment like Egypt, the linear dunes are dominant (Breed et al., 1979; Tsoar, 1978). However, limited studies have been carried out on the migration rates of the linear dunes in Egypt as a whole (Embabi, 2004), and in Sinai Peninsula in particular (ElBanna, 2004; Khidr, 2006). Table (3) presents the previous studies that were carried out on linear dunes in north Sinai Peninsula. Except for ElBanna (2004) who made a comparison between an aerial photograph acquired in 1958 and a LandSat ETM image acquired in 1998, all the previous measurements were carried out either on a single or two linear dune(s) in north Sinai. The majority of these measurements had been carried out on the lateral movements of the crest line and the elongation of the linear dunes whereas a limited number of measurements were carried out on the longitudinal displacements of the peaks and saddles of the linear dunes (Table 3). The lateral movements along the crest lines of the linear dunes ranged from 0.7 to 10.6 m/yr with an average of 5.2 m/yr. The elongation of the studied dunes ranged from 2.3 to 27.0 m/yr with an average of 12.9 m/yr whereas the longitudinal displacement of peaks and saddles of these dunes ranged from 7.5 to 10.9 m/yr with an average of 8.8 m/yr. The wide range of these measurements may be attributed to the different locations of the studied

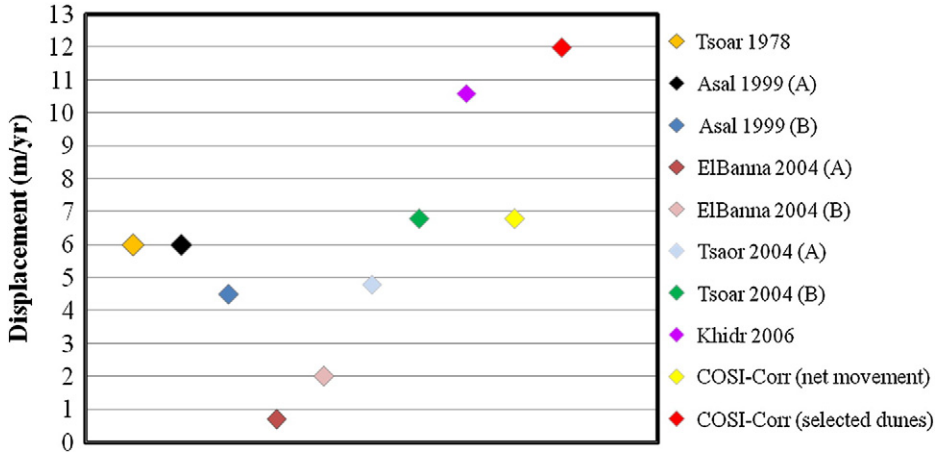

Fig. 8. Validation of pixel displacement of the linear dunes against the lateral measurements of the previously studied linear dunes. Asal, 1999 and ElBanna, 2004 (A and B) means two different dunes, Tsoar et al., 2004 (A and B) refers two measurements at two time intervals for the same linear dunes.

dunes and the various techniques used in the measurements, along with the time interval of monitoring.

Unlike field techniques and the fine resolution aerial photographs used in the previous studies (Tsoar, 1978; Tsoar et al., 2004), the SPOT 4 images with spatial resolution of 10.0 m used in this study cannot help identify the precise locations of dune ends. Accordingly, determination of elongation movements at the end of the linear dunes would be hard. However, the lateral displacements along crest lines could be recognized and measured using these images (Fig. 7). From this perspective, the majority of the measured pixel displacements express the lateral displacements of the peaks and saddles along the crest lines of the linear dunes. The values of the lateral pixel displacements of the linear dunes in entire area of study are in the order of 4.2 to 20.10 m/yr with a net average of 6.8 m/yr. However, these displacements vary from a linear dune to another, and along the crest lines of each linear dune as well. Two profiles were made in a selected area of linear dunes (Fig. 7I): one across different linear dunes (Fig. 7II) and another one along a selected linear dune (Fig. 7III). The first profile passes through a number of peaks and saddles of different dunes and the interdune areas over a whole distance of 250 m whereas the second profile passes through all the peaks and saddles of 200.0 m long linear dune. The first profile shows high oscillation of pixel displacements not only between dunes and the interdune areas but also between peaks (P) and saddles (S) of different dunes. The high displacements are associated with the peaks and saddles whereas the low displacements are associated with the interdune areas. The pixel displacement of the peaks of the different linear dunes range from 12.0 to 15.5 m/yr with an average of 13.4 m/yr whereas the pixel displacements of the saddles are on the order of 11.0 to 16.0 m/yr with an average of 13.0 m/yr (Fig. 7II). The second profile reveals an additional characteristic of the lateral movements of the linear dunes where the lateral pixel displacements significantly varies among peaks and saddles along the same linear dune (Fig. 7III). The range of these displacements is on the order of 5.5 to more than 16.7 m/yr with an average of 12.4 m/yr. This wide range expresses high variability of the lateral movements of the peaks and saddles along the crest line of the same linear dune. This aspect had been recorded by Tsoar (1978), Tsoar (1983), Tsoar et al. (2004), Asal (1999), ElBanna (2004), and Khidr (2006). The saddles are longer, and move relatively faster than the peaks. The pixel displacement of

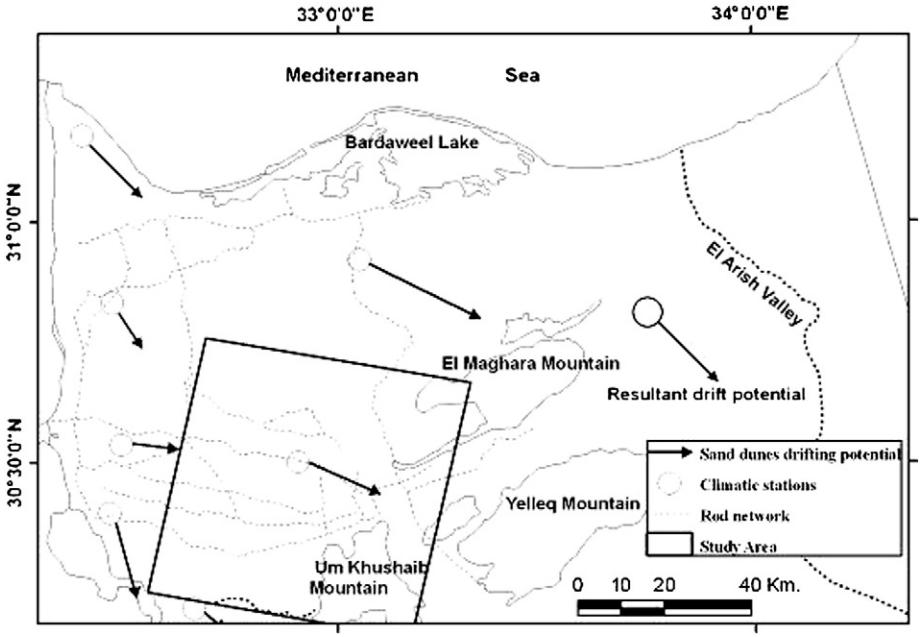

Fig. 9. Sand dunes drifting potential in north Sinai; modified after ElBanna (2004).

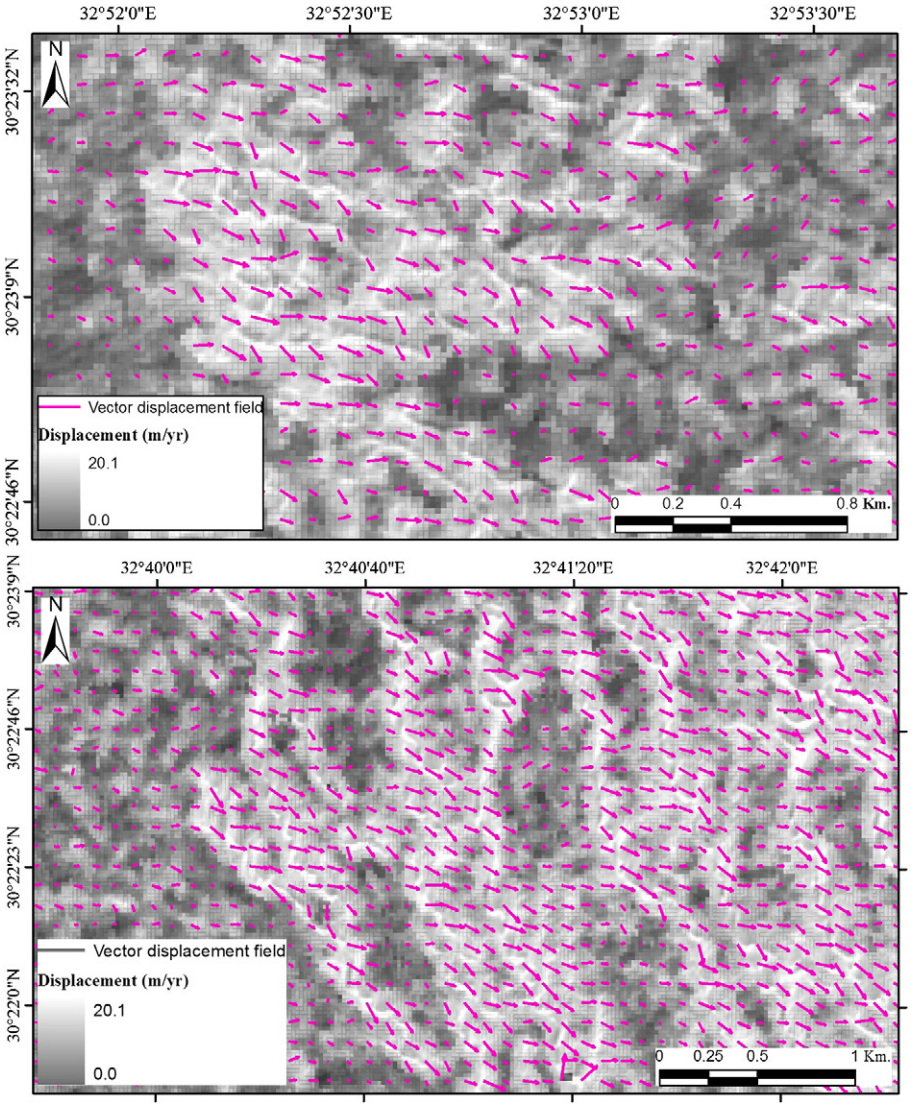

Fig. 10. the vector displacement field displayed over the calculated net pixel displacement image.

saddles along the studied linear dune (Fig. 7III) ranged from 12.0 to 14.8 m/yr with an average of 13.1 m/yr whereas the lateral pixel displacement of the peaks ranged from 5.5 to 16.7 m/yr with an average of 11.6 m/yr (Fig. 7III). Validation of the measured lateral movement of the linear dunes of the whole studied area (net lateral migration) and the selected profile against the previously measured lateral movements of linear dunes in north Sinai is given in Fig. (8). The figure indicates that the estimated lateral movements of the linear dunes by the COSI-Corr technique are comparable to the estimated values of the previous studies. Given that the linear dunes are characterized by considerable lengths extending hundreds or thousands of meters, and may be thousands of kilometers (Bagnlod, 1941; King, 1960; Twidale, 1972; Wilson, 1972) making field measurements impossible, the current technique is a potential alternative to provide accurate measurements of a large fields of linear dunes.

4.3. Direction of sand dune movements

North Sinai belongs to complex wind systems. Most of the previous works that have been carried out on sand dune movements in north Sinai analyzed wind parameters that control sand dune formation and movements such as direction and magnitude (Aql, 2002; Asal, 1999; ElBanna, 2004; ElDessouki, 2000; Hereher, 2000; Khidr, 2006) using the meteorological stations. Wind direction and wind speed are the main characteristics that control the aeolian processes. The dominant wind directions in the study area are the northwestern, northern, and northeastern directions. They vary slightly from season to season. Wind speed is an important characteristic that initiates the aeolian processes. ElBanna (2004) applied Zenda et al. (1988) model to identify the relationship between the effective wind velocity (threshold) and the grain size diameter. Applying this relationship, ElBanna (2004) concluded that the effective wind speed that can entrain and carry the dominant grain size of the study area is 4.0 m s^{-1} (7.8 knots h^{-1}). As the dominant wind speed is higher than this value (ElBanna, 2004), the study area receives high percentages of the effective winds that can entrain and carry sands. The percentages of the effective winds vary seasonally (ElDessouki, 2000). It increases in summer (~50%) and spring (~46%) and decreases in autumn (~40%) and winter (~25%). In addition, ElBanna (2004) and Hereher (2000) calculated the sand dune drifting potential seasonally and annually. Both concluded that the movement of sand occurs in the southeast and east directions (Fig. 9) in response to the dominant stronger winds blowing from the northwest and west. These conclusions are highly related to the result of the estimated displacement fields from the current technique.

One of the outcomes from the sub-pixel correlation technique is the vector displacement field that determines the direction of pixel displacement. The vector displacement field was produced by combing both the east–west and the north–south displacement components. Each arrow

comprises an arc segment where its length is an indicator of the amount of movement, and the head of the arrow refers to the direction of movement. The lengths of the arrows are longer over the dunes and shorter over the interdune areas (Fig. 10I and II). The direction of the arrows indicates that the direction of pixel displacements occur in the southeastern to the eastern directions which is consistent with the direction of wind regime and the calculated sand dune drifting potential.

5. Conclusion

Unlike the traditional techniques using field measurements and remote sensing, the sub-pixel correlation technique can provide measurements of sand dune movement over wider spatial coverage at high accuracy. Applying this technique, it was possible to identify three spatial characteristics of sand dunes in the studied areas which are the spatial distribution of sand dunes relative to other morphologic units in the study area, the magnitude of the migration rates, and the direction of these migrations. The technique had differentiated well between the movable sand dune areas and the stable interdunal areas. The magnitude of the lateral migration and directions of both barchan and linear dunes were estimated and validated against the previously measured migration rates and directions. The validation indicated that the results of the current technique are highly comparable with the previous results. However, the current technique has the privilege of providing the lateral migration rates and directions over wide spatial coverage which allows studying the spatial variability of dune migration. This information is especially valuable when monitoring the linear dunes, which could extend for long distances and that represent a real challenge to field techniques. Given these aspects, the sub-pixel correlation of satellite imagery is considered a new perspective to study sand dune hazards in north Sinai. The determination of the rates and direction of sand dune migration over wide spatial coverage and at sub-pixel accuracy can help define the road segments that are under potential risk of dune migration. In addition, alternative safe corridors for specific time scale can be defined. However, these issues could be extended using the results of this study through other research activities.

Acknowledgment

The authors would like to thank the National Authority for Remote Sensing and Space Sciences (NARSS) for supporting this research activity through providing satellite imagery and funding the field work. S. Leprince was partly supported by the Keck Institute for Space Studies and by the Gordon and Betty Moore Foundation.

References

Aql, M. T. (2002). Movement of sands east Suez Canal and its impact on human activities: A study in applied geomorphology (In Arabic). *Al-Ensaniat*, *19*, 1–75.

Asal, M. E. (1999). Sedimentological studies on the Quaternary sand dunes and sabkhas, Northern Sinai, Egypt. MSc. Thesis, Geology Department (Domyat), Mansoura University, Egypt.

Avouac, J., Ayoub, F., Leprince, S., Konca, O., & Helmberger, D. V. (2006). The 2005, Mw 7.6 Kashmir earthquake: Sub-pixel correlation of ASTER images and seismic waveforms analysis. *Earth and Planetary Science Letters*, *249*, 514–528.

Ayoub, F., Leprince, S., & Avouac, J. (2009). Co-registration and correlation of aerial photographs for ground deformation measurements. *ISPRS Journal of Photogrammetry and Remote Sensing*, *64*, 551–560.

Bagnlod, R. A. (1941). *The physics of blown sand and desert dunes.* London: Chapman & Hall 256 pp.

Breed, C. S., Fryberger, S. G., Andrews, S., McCauley, C., Lennartz, F., Gebel, D., et al. (1979). Regional studies of sand seas using Landsat (ERTS) imagery. In E. D. McKee (Ed.), *A study of global sand seas. Prof. Pap. U.S. Geol. Surv., 1052*. (pp. 305–397).

Buades, A., Coll, B., & Morel, J. M. (2008). Non local image and movie denoising. *International Journal of Computer Vision*, *76*(2), 123–139.

COSI-CORR User's Guide (2009). *Co-registration of optically sensed images and correlation.* USA: California Institute of Technology.

ElBanna, M. S. (1999). Geological studies of sand dunes of El-Sheikh Zuweid area, East of Wadi El-Arish, north Sinai, Egypt. MSc: Dissertation, Department of Geology, Cairo University, Egypt.

ElBanna, M. S. (2004). Geological studies emphasizing the morphology and dynamics of sand dunes and their environmental impacts on the reclamation and developmental areas in northwest Sinai, Egypt. PhD Dissertation, Department of Geology, Cairo University, Egypt.

ElDessouki, S. A. (2000). Longitudinal dunes east Suez Canal: A geomorphic analysis (In Arabic). *Bulletin De La Société De Géographie D'égypte*, *35*, 231–280.

ElKayali, M. (1984). Geomorphologic studies of the coastal plain, north Sinai Peninsula. PhD Thesis, Ain Shams University.

Embabi, N. (2004). The geomorphology of Egypt: Landforms and evolution. *The Nile Valley and the Western Desert*, *vol 1*, Shobra, Cairo, Egypt: Nubar Printing House.

Hereher, M. (2000). A study on sand dunes fields in north Sinai and the environmental risk assessment of Aeolian processes. MSc Thesis, Faulty of Science (Dumyat), Mansoura University, Egypt.

Khalaf, F. I., Zaghloul, E. A., & Hereher, M. (1998). Sedimentomorphic classification of the NW Sinai dune fields as revealed by the satellite images. *Egyptian Journal of Remote Sensing and Space Sciences*, *1*, 165–194.

Khidr, M. (2006). Aeolian forms and their hazards in the west of Wadi El-Arish: A geomorphological study. PhD Dissertation, Geography Department, Ain Shams University, Egypt.

King, D. (1960). The sand ridge deserts of South Australia and related Aeolian landforms of the quaternary and arid cycles. *Transactions of the Royal Society of South Australia*, *83*, 99–108.

Leprince, S., Barbot, S., Ayoub, F., & Avouac, J. (2007). Automatic and precise orthorectification, coregistration, and subpixel correlation of satellite images, application to ground deformation measurements. *IEEE Transactions on Geoscience and Remote Sensing*, *45*(6), 1529–1558.

Liu, J. G., Capes, R., Haynes, M., & Moore, J. M. (1997). ERS SAR multi-temporal coherence image as a tool for sand desert study (sand movement, sand encroachment and erosion). *The Twelfth International Conference and Workshop on Applied Geologic Remote Sensing, Denver, Colorado* (pp. I-478–I-485).

Liu, J. G., Mason, P. G., & Ma, J. (2006). Measurement of the left lateral displacement pf Ms 8.1 Kunlun earthquake on 14 November 2001 using Landsat ETM + imagery. *International Journal of Remote Sensing*, *27*(10), 1875–1891.

Madigan, C. T. (1946). The Simpson Desert Expedition, 1939 scientific reports: no. 6, geology—The sand formation. *Transactions of The Royal Society of South Australia*, *70*, 45–63.

Michel, R., & Avouac, J. P. (2002). Deformation due to the 17 August 1999 Izmit, Turkey, earthquake measured from SPOT images. *J. Geophys. Res.*, *107*(B4), p. 2062.

Misak, R. F., & ElShazly, M. (1982). Studies on blown sand at some localities in Sinai and northern desert, Egypt. *Journal of Geology*, *special issue 1*, 115–131.

Mounir, M. M. (1983). *Sand dunes in Egypt.* Cairo, Egypt: Academy of Scientific Research and Technology 175 pp.

Necsoiu, M., Leprince, S., Hooper, D. M., Dinwiddie, C. L., McGinnis, R. N., & Walter, G. R. (2009). Moniktoring migration rates of an active subarctic dune field using optical imagery. *Remote Sensing of Environment*, *113*, 2441–2447.

Scherler, D., Leprince, S., & Strecker, M. R. (2008). Glacier-surface velocities in alpine terrain from optical satellite imagery — Accuracy improvement and quality assessment. *Remote Sensing of Environment*, *112*, 3806–3819.

Schiek, C. G. (2004). Terrain change detection using aster optical satellite imagery along the Kunlun Fault, Tibet. A PhD Thesis, Department of the Geological Sciences, The University of Texas At ElPaso.

Schiek, C. G., & Hurtado, J. M., Jr. (2006). Slip analysis of the Kokoxili earthquake using terrain change detection and regional earthquake data. *Geosphere*, *2*(3), 187–194.

Tsoar, H. (1974). Desert dunes morphology and dynamics, El Arish, Northern Sinai. *Zeitschrift fur Geomorphologie, Supplement Band*, *20*, 41–61.

Tsoar, H. (1978). The dynamics of longitudinal dunes. *Final Technical Report, European Research Office, U.S. Army, London* 171 pp.

Tsoar, H. (1983). Dynamic processes acting on a Longitudinal Seif sand Dunes. *Sedimentology*, *30*, 567–578.

Tsoar, H. (1984). The formation of seif dunes from barchans — A discussion. *Zeitschrift für Geomorphologie Supplementband N.F.*, *28*(1), 99–103.

Tsoar, H. (1989). Linear dunes — Forms and formation. *Progress in Physical Geography*, *13*, 507–528.

Tsoar, H., Blumberg, D. G., & Stoler, Y. (2004). Elongation and migration of sand dunes. *Geomorphology*, *57*, 293–302.

Twidale, C. R. (1972). Evoluation of sand dunes in the Simpson Desert, Central Australia. *Transactions of the Institute of British Geographers*, *56*, 77–106.

Van Puymbroeck, N., Michel, R., Binet, R., Avouac, J. P., & Taboury, J. (2000). Measuring earthquakes from optical satellite images. *Applied Optics*, *39*(20), 3486–3494.

Vermeesch, P., & Drake, N. (2008). Remotely sensed dune celerity and sand flux measurements of the world's fastest barchans (Bodele, Chad). *Geophysical Research Letters*, *35*, L24404 6 PP.

Wilson, I. G. (1972). Aeolian landforms — Their development and origins. *Sedimentology*, *19*, 173–210.

Zenda, Z. Z., Benggony, D., Xinmin, W., Kangfu, & Jixian, D. (1988). Desertification and and rehabilitation case study in Horgin sand land. *Inst. Desert-Res., Academic Sincia, Lnzhou, China* (pp. 14–49).